

# A COMPARATIVE STUDY ON POOL BOILING OF FC-72 ON MICRO-PIN-FIN SILICON SURFACES WITH AND WITHOUT NANOPARTICLES

Zhen Cao<sup>1</sup>, Bin Liu<sup>2</sup>, Zan Wu<sup>1</sup>, Yonghai Zhang<sup>2</sup>, Jinjia Wei<sup>2</sup>, Bengt Sundén<sup>1\*</sup>

<sup>1</sup> Department of Energy Sciences, Lund University, Lund, Sweden

<sup>2</sup> School of Chemical Engineering and Technology, Xi'an Jiaotong University, Xi'an, China

## ABSTRACT

Several methods have been developed to enhance boiling heat transfer by surface modification, e.g., mechanical methods, chemical methods and hybrid methods. In the present study, micro-pin-fin silicon surfaces are prepared by a dry etching method. Subsequently, the micro-pin-fin surfaces are deposited with copper nanoparticles (20±5 nm) by an electrostatic deposition method. Saturated pool boiling heat transfer of FC-72 is experimentally investigated, illustrating the effect of nanoparticles on the saturated pool boiling heat transfer. Compared with the micro-pin-fin surface, the nanoparticles have slight effects on the heat transfer at low heat fluxes (< 5 W/cm<sup>2</sup>), while at moderate-high heat fluxes (>5 W/cm<sup>2</sup>), the effect of nanoparticles depends on the deposition time. In the present case, heat transfer is deteriorated on the micro-pin-fin surface with 1h deposition at moderate-high heat fluxes, but the heat transfer is slightly enhanced at moderate heat fluxes (5 - 15 W/cm<sup>2</sup>) and is slightly deteriorated at high heat fluxes (>15 W/cm<sup>2</sup>) on the micro-pin-fin surface with 2h deposition. Additionally, compared with the micro-pin-fin surface, the critical heat flux (CHF) is slightly enhanced (around 7%) on the micro-pin-fin surface with 2h deposition, but is almost the same on the micro-pin-fin surface with 1h deposition. To study the reasons behind these results, SEM images are taken to characterize the surfaces and high speed visualization is conducted to compare bubble behaviors. In addition, supplementary experiments are designed to measure the wickability on these surfaces.

**Keywords:** pool boiling, nanoparticle, critical heat flux, heat transfer

## NONMENCLATURE

### *Abbreviations*

CHF	critical heat flux, W/cm <sup>2</sup>
HTC	heat transfer coefficient, W/cm <sup>2</sup> K
MPFS	micro-pin-fin surface
NP	nanoparticle

### *Symbols*

$A_c$	cross section area of the capillary tube, m <sup>2</sup>
$q$	heat flux, W/cm <sup>2</sup>
$T$	temperature, K
$\Delta T$	superheat, K

## 1. INTRODUCTION

Thermal management is a big issue in many applications, e.g., electronics, solar power plants and internal combustion engine. For example, as reported by Intel company, the thermal design power of the Intel processor increases from 104 W (Intel Core i3 540) to 174 W (Intel Core i7 975), and the size of the transistor decreases from 90 nm in 2004 to 10 nm in 2017 [1]. This results in high-heat-flux surfaces that need to be cooled down, e.g., 95 - 110 W on the surface of 13.52×9.05 mm<sup>2</sup> in the Intel Core i7-6700 K [2]. The traditional cooling technology, i.e., air cooling, has difficulties to meet the cooling demand, while boiling heat transfer is a potential method due to its high heat transfer performance with a small superheat. Therefore, it has attracted much attention to enhance the performance of boiling heat transfer.

Up to date, numerous methods have been used to modify surfaces to enhance boiling performance, e.g., dry etching [2, 3], wire electrical discharge machining (WEDM) [4], sintering [5 - 7], laser technique [8 - 10] and surface deposition [11, 12]. For examples, Kong et al. [2] studied pool boiling of FC-72 on a smooth silicon surface, a micro-pin-fin surface and bistructured surfaces. It was found that the bistructured surfaces performed better than others, i.e., higher heat transfer coefficients and CHF. Waluni and Sathvabhama [4] investigated pool boiling performance with distilled on copper surfaces by WEDM. It was found that the incipient temperature was reduced by 13.7% - 23.2% and the heat transfer coefficient increased by 21.5% - 35.4%. NaserSharifi et al. [5] studied pool boiling enhancement of N-pentane using a multilevel modulated wick fabricated by sintering. A 250% CHF improvement was achieved. Tang et al. [7] combined the WEDM and sintering to generate porous interconnected microchannel nets on copper surfaces which exhibited a lower wall-superheat at the onset of water nucleate boiling (ONB) and a 22% higher nucleate boiling heat transfer coefficient (HTC) than the solid interconnected microchannel net. Wong and Leong [9] obtained a CHF 2.8 times that of the smooth surface with FC-72 on surfaces by the selective laser melting. In fact, the methods above depend on expensive facilities. Nowadays, many coating technologies are employed, which are cheap and easy-operation. Xu et al. [11] studied the boiling performance of DI water on coating surfaces by an electrochemical deposition method. It was shown that the critical heat flux (CHF) increased with surface wettability and coating thickness, while the effect of the surface wettability on nucleate boiling heat transfer was complicated. Jo et al. [12] compared the effects of capillarity on pool boiling of water using nano-textured surfaces by electrospayed BiVO<sub>4</sub> nano-pillars. It was found that the heat transfer coefficient and critical heat flux could both be enhanced, but the CHF did not increase with increasing electrospaying time.

As discussed above, numerous studies have been devoted to enhance boiling performance by manufacturing micro/nano structures. This study aims to investigate the further effects of nanoparticles on the boiling performance on a micro-pin-fin silicon surface. Saturated pool boiling heat transfer of FC-72 was experimentally studied on a smooth silicon surface, a micro-pin-fin surface and two micro-pin-fin surfaces with nanoparticles.

## 2. EXPERIMENTAL STUDIES

### 2.1 Test surfaces

In the present study, the micro-pin-fin surface was prepared by a dry etching method. Afterwards, the nanoparticles were deposited on the micro-pin-fin surfaces by an electrostatic deposition method, varying the deposition time. The present micro pin fins are square and are arranged in a staggered pattern, as shown in Fig. 1(a). Table 1 summarizes the test surfaces, in which SS, MPFS, MPFS-NP-1h and MPFS-NP-2h represent the smooth surface, the micro-pin-fin surface, the micro-pin-fin surface with 1h deposition and the micro-pin-fin surface with 2h deposition, respectively. More details about the surface preparation are available in our previous study [13]. The test rig, test procedure and data reduction are also available in [13]. The maximum uncertainties of  $q$  and HTC are estimated as 6% and 6.3%, respectively, in the nucleate boiling regime.

Table 1 test surfaces

Surfaces	w ( $\mu\text{m}$ )	h ( $\mu\text{m}$ )	p ( $\mu\text{m}$ )	deposition time
SS	*	*	*	*
MPFS	30	60	45	*
MPFS-NP-1h	30	60	45	1h
MPFS-NP-2h	30	60	45	2h

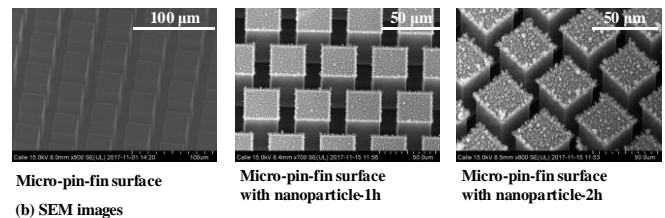
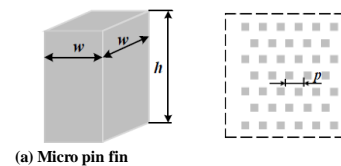


Fig 1 Surface characteristics: (a) the SS (smooth surface) after polishing; (b) SEM image of EPD-0.25mg before experiments

The micro-pin-fin surface and the surfaces with nanoparticles were characterized by a Scanning Electron Microscope (Hitachi SU8010), as shown in Fig. 1(b). It is shown that the micro pin fins are laid out in a staggered pattern precisely. The nanoparticles are almost deposited on the top surfaces of the micro pin fins, instead of the side surfaces and the bottom. Due to the various deposition time, it is obvious that the surface with a longer-time deposition exhibits more

nanoparticles. Actually, many studies show that bubbles prefer to nucleate on the side-bottom corner of pin fins, instead of the top surface [14, 15]. However, the nanoparticles almost concentrate on the top surface. It is interesting to study the effect of this deposition on the boiling performance.

## 2.2 Results and discussion

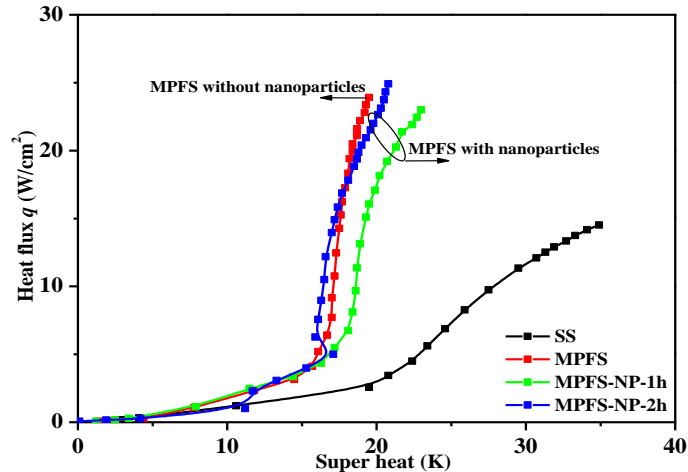


Fig 2 Boiling curves of the smooth and modified surfaces

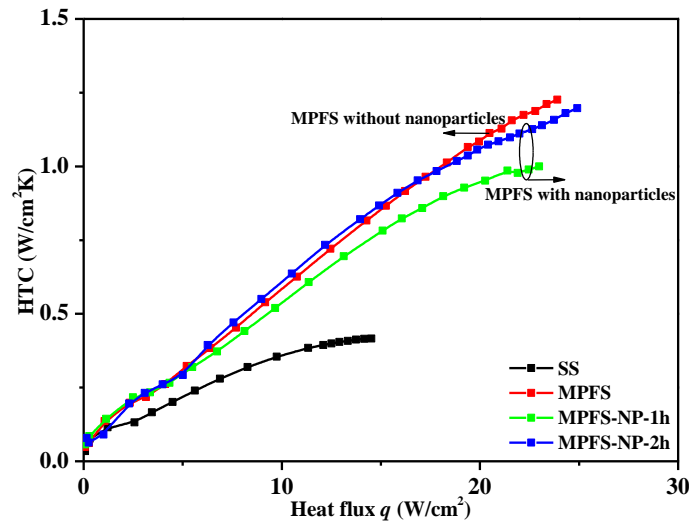


Fig 3 Heat transfer coefficient comparison between the smooth surface and modified surfaces

Figure 2 shows the boiling curves of the SS, MPFS, MPFS-NP-1h and MPFS-NP-2h. It is obvious that the boiling curves of the non-smooth surfaces move to the left compared with that of the smooth surface. The maximum superheat can be reduced by around 15 K. The maximum superheat on the MPFS, MPFS-NP-1h and MPFS-NP-2h are 19.5 K, 23.0 K and 20.8 K, respectively, while the maximum superheat on the SS is 34.9 K. The left-shifting boiling curves mean that the heat transfer is enhanced by the micro pin fins and nanoparticle deposition. In terms of the CHF, it is significantly

enhanced on the non-smooth surfaces, compared with the smooth surface. However, the nanoparticles seem not to further enhance the CHF considerably, in comparison to the micro-pin-fin surface. For example, the CHFs on the MPFS, MPFS-NP-1h and MPFS-NP-2h are 23.9 W/cm<sup>2</sup>, 23.0 W/cm<sup>2</sup> and 24.9 W/cm<sup>2</sup>, respectively, while the CHF on the SS is 14.5 W/cm<sup>2</sup>. More discussion about the CHF will be provided later.

Figure 3 compares the heat transfer coefficient of the test surfaces. Compared with the SS, the heat transfer coefficient can be enhanced by around 70% on the non-smooth surfaces. However, compared with the micro-pin-fin surface, the effect of nanoparticles on the heat transfer coefficient is almost negative in this case. At low heat fluxes (< 5 W/cm<sup>2</sup>), the nanoparticles have slight effects on the heat transfer, compared with the micro-pin-fin surface, while at moderate-high heat fluxes (>5 W/cm<sup>2</sup>), the effect of nanoparticles depends on the number of the nanoparticles, i.e., heat transfer is deteriorated on the micro-pin-fin surface with 1h deposition, but the heat transfer is slightly enhanced at moderate heat fluxes (5 - 15 W/cm<sup>2</sup>) and is slightly deteriorated at high heat fluxes (>15 W/cm<sup>2</sup>) on the micro-pin-fin surface with 2h deposition. The heat transfer coefficient should depend on the active nucleation site density and bubble dynamics. On one hand, probably, the nanoparticles make the surface more hydrophilic. This leads to more difficult nucleation according to the classical nucleation theory. Also as shown in the SEM images, nanoparticles almost laid on the top surface of the micro pin fin, which probably contribute little to the active nucleation site density. Conversely, on the other hand, the more hydrophilic surface due to nanoparticle deposition probably has smaller bubble departure diameter and larger bubble frequency, according to some bubble departure diameter models, e.g., Fritz [16]. Then the comprehensive effect of nanoparticles depend on the trade-off between these two aspects. Here, it is postulated that the heat transfer can be further enhanced by nanoparticles if the nanoparticles are deposited for longer time and more nanoparticles lay on the side surfaces and bottoms of the micro pin fins.

Figure 4 compares the bubble behavior on the test surfaces at high heat fluxes approaching the CHF. It is found that the bubble behavior is different between the SS and the non-smooth surfaces. On the SS as shown in Fig. 4(a), a vapor blanket is formed on the surface. The bubbles rise from the vapor blanket and then depart from the surface. The vapor interface was captured,

indicated by the red dashed line. The vapor interface exhibits a quasi - sinusoidal shape, which is consistent with the CHF triggering mechanism proposed by Zuber [17]. It is deduced that the CHF mechanism on the SS is due to the hydrodynamic instability. When the heat flux reaches the CHF, the vapor collapses on the surface, preventing any liquid supply. Regarding the CHF on the MPFS, MPFS-NP-1h and MPFS-NP-2h, the CHF mechanism is more or less different from that on the SS, validated by the bubble visualization as shown in Fig. 4(b-c). On the non-smooth surfaces, the patches exposed in the liquid can be recognized, indicated by the red arrow, although the dryout patches become larger and larger as time passes. Actually, numerous studies already investigated the mechanism of CHF enhancement on non-smooth surfaces, e.g., Kim et al. [18] and Kwark et al. [19] contributed the CHF enhancement to the capillary wicking on micro-pillar surfaces and nanocoated surfaces, respectively. Cao et al. [13] and Zhou et al. [20] also proposed that the CHF enhancement was due to the wickability measured by the method proposed by Rahman et al. [21].

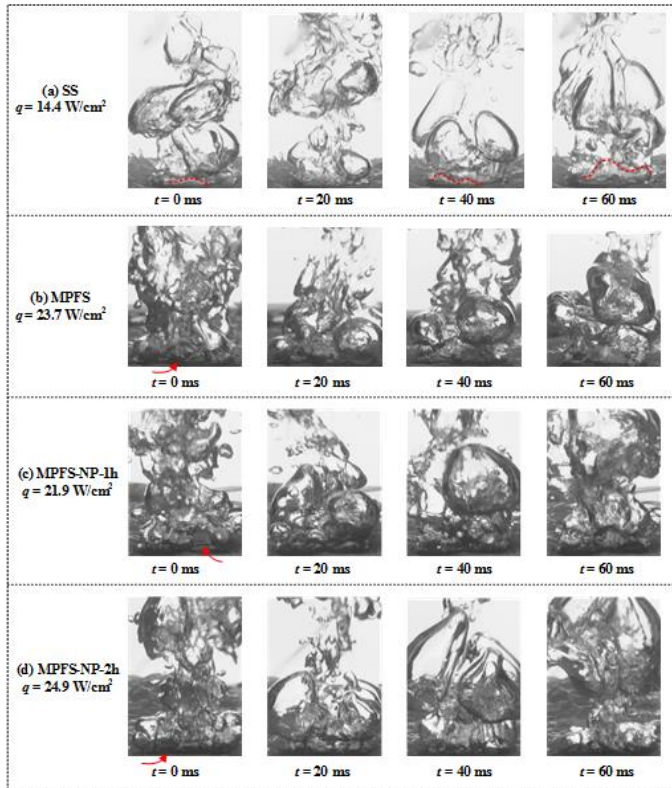


Fig 4 Bubble dynamics at high heat fluxes approaching CHF

In the present study, the wickability was also measured, which is characterized by

$$V' = \frac{dV}{dt} = \frac{A_c dl}{dt} \quad (1)$$

where  $A_c$  is the area of the cross section of the micro-capillary tube.  $h$  is the height of the liquid in the micro-capillary tube.

Figure 5 compares the height change of the liquid with time, which can characterize the wickability of the surfaces. In another word, better wickability means quicker liquid absorption on the surface, representing a larger curve slope in Fig. 5. Obviously, the wickability is greatly enhanced on the MPFS, the MPFS-NP-1h and the MPFS-NP-2h, compared with the SS. Therefore, the CHF is enhanced.

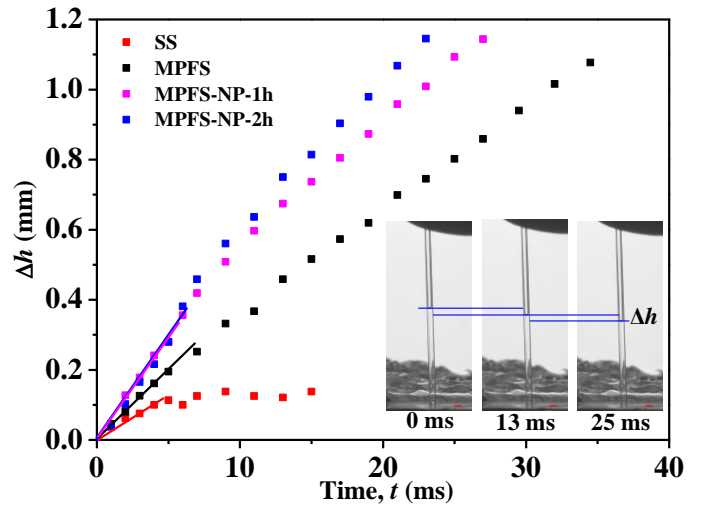


Fig 5 The height change of the liquid with time (scale bar: 0.6 mm).

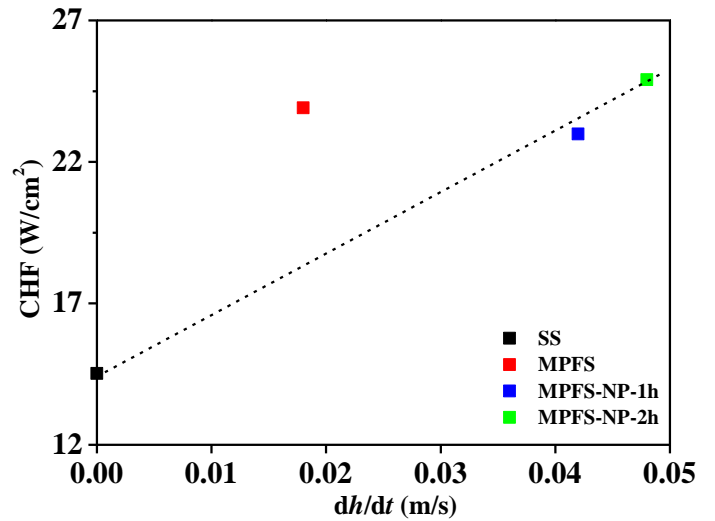


Fig 6 The relationship between wicking velocity and CHF of different surfaces.

The relationship between the CHF and the wicking velocity is shown in Fig. 6 in which the wicking velocity of the SS is considered to be zero, while the wicking velocities of other surfaces are the net wicking velocities which are the increased compared with the SS. It can be seen that the wicking velocity has a good linear

relationship with the CHF, which shows that the capillary wickability of the surface is one of the most significant factors affecting the CHF. However, it is evident that the CHF of MPFS deviates from the dashed line, which is consistent with the result in [20], saying that the CHF on the MPFS is also affected by other mechanisms besides the wickability. For example, probably the liquid supply is not only dominated by the liquid wicking, but also dominated by the time gap between the large bubble departure and the next bubble occurrence. Maybe, this time gap is large on the MPFS, which enhances the CHF considerably.

### 2.3 Conclusions

Experiments of saturated pool boiling were conducted with FC-72 at atmospheric pressure on a smooth silicon surface (SS), a micro-pin-fin surface (MPFS) and two micro-pin-fin surfaces with nanoparticles (MPFS-NP-1h and MPFS-NP-2h). The boiling curves and heat transfer coefficients were compared. Bubble behaviors were captured by a high speed camera at low, moderate and high heat fluxes. Possible mechanisms for the CHF enhancement were discussed. Several conclusions are summarized as follows:

- Compared with the SS, the maximum superheat can be reduced by around 15 K on the MPFS, MPFS-NP-1h and MPFS-NP-2h.
- Compared with the SS, the heat transfer coefficient can be enhanced by around 70% on the MPFS, MPFS-NP-1h and MPFS-NP-2h.
- Compared with the MPFS, the effect of the nanoparticles on the heat transfer coefficient depends on the deposition time and the heat flux. However, it is postulated that a longer deposition time can further enhanced the heat transfer.
- In terms of the CHF, it is significantly enhanced on the MPFS, MPFS-NP-1h and MPFS-NP-2h, compared with the SS. However, the nanoparticles seem not to further enhance the CHF considerably, in comparison to the MPFS. For example, the CHFs on the MPFS, MPFS-NP-1h and MPFS-NP-2h are  $23.9 \text{ W/cm}^2$ ,  $23.0 \text{ W/cm}^2$  and  $24.9 \text{ W/cm}^2$ , respectively, while the CHF on the SS is  $14.5 \text{ W/cm}^2$ .
- The CHF enhancement is contributed to the wickability. Compared with the SS, the wickability is considerably improved on the MPFS, MPFS-NP-1h and MPFS-NP-2h.

### ACKNOWLEDGEMENT

The work is done in Xi'an Jiaotong University, supported by a STINT-NSFC joint project and the Swedish

Scientific Council (VR). Zhen Cao thanks The China Scholarship Council (CSC) for the PhD study scholarship.

### REFERENCE

- [1] <https://www.anandtech.com/show/4083/the-sandy-bridge-review-intel-core-i7-2600k-i5-2500k-core-i3-2100-tested/21>
- [2] Kong X, Zhang Y, Wei JJ. Experimental study of pool boiling heat transfer on novel bistructured surfaces based on micro-pin-finned structure. *Exp Therm Fluid Sci* 2018;91:9-19.
- [3] Liu Y, Lu MC, Xu D. The suppression effect of easy-to-activate nucleation sites on the critical heat flux in pool boiling. *Int J Therm Sci* 2018;129:231-237.
- [4] Walunj A, Sathyabhama A. Comparative study of pool boiling heat transfer from various microchannel geometries. *Appl Therm Eng* 2018;128:672-683.
- [5] Nasersharifi Y, Kaviany M, Hwang G. Pool-boiling enhancement using multilevel modulated wick. *Appl Therm Eng* 2018;137:268-276.
- [6] Ji X, Xu J, Zhao Z, Yang W. Pool boiling heat transfer on uniform and non-uniform porous coating surfaces. *Exp Therm Fluid Sci* 2013;48:198-212.
- [7] Tang Y, Zeng J, Zhang S, Chen C, Chen J. Effect of structural parameters on pool boiling heat transfer for porous interconnected microchannel nets. *Int J Heat Mass Transfer* 2016;93:906-917.
- [8] Zhang C, Zhang L, Xu H, Li P, Qian B. Performance of pool boiling with 3D grid structure manufactured by selective laser melting technique. *Int J Heat Mass Transfer* 2019;128:570-580.
- [9] Wong KK, Leong KC. Saturated pool boiling enhancement using porous lattice structures produced by Selective Laser Melting. *Int J Heat Mass Transfer* 2018;121:46-63.
- [10] Liu B, Cao Z, Zhang Y, Wu Z, Pham A, Wang W, Yan Z, Wei J, Sundén B. Pool boiling heat transfer of N-pentane on micro/nanostructured surfaces. *Int J Therm Sci* 2018;130:386-394.
- [11] Xu P, Li Q, Xuan Y. Enhanced boiling heat transfer on composite porous surface. *Int J Heat Mass Transfer* 2015;80:107-114.
- [12] Jo HS, Kim MW, Kim K, An S, Kim YI, James SC, Choi J, Yoon SS. Effects of capillarity on pool boiling using nano-textured surfaces through electrosprayed BiVO<sub>4</sub> nano-pillars. *Chem Eng Sci* 2017;171:360-367.
- [13] Cao Z, Liu B, Preger C, Wu Z, Zhang Y, Wang X, Messing ME, Deppert K, Wei J, Sundén B. Pool boiling heat transfer of FC-72 on pin-fin silicon surfaces with nanoparticle deposition. *Int J Heat Mass Transfer* 2018;126:1019-1033.

- [14] Walunj A, Sathyabhama A. Comparative study of pool boiling heat transfer from various microchannel geometries. *Appl Therm Eng* 2018;128:672-683.
- [15] Wei JJ, Honda H. Effects of fin geometry on boiling heat transfer from silicon chips with micro-pin-fins immersed in FC-72. *Int J Heat Mass Transfer* 2003;46:4059-4070.
- [16] Collier JG, Thome JR. Convective boiling and condensation. 3<sup>rd</sup> ed. Oxford University Press; 1994.
- [17] Zuber N. Hydrodynamic aspects of boiling heat transfer (Thesis). United States; 1959.
- [18] Kim SH, Lee GC, Kang JY, Moriyama K, Kim MH, Park HS. Boiling heat transfer and critical heat flux evaluation of the pool boiling on micro structured surface. *Int J Heat Mass Transfer* 2015;91:1140-1147.
- [19] Kwark SM, Moreno G, Kumar R, Moon H, You SM. Nanocoating characterization in pool boiling heat transfer of pure water. *Int J Heat Mass Transfer* 2010;53:4579-4587.
- [20] Zhou J, Liu B, Qi B, Wei J, Mao H. Experimental investigations of bubble behaviors and heat transfer performance on micro/nanostructure surfaces. *Int J Therm Sci* 2019;135:133-147.
- [21] Rahman MM, Olceroglu E, McCarthy M. Role of wickability on the critical heat flux of structured superhydrophilic surfaces. *Langmuir* 2014;30:11225-11234.